J|A|C|S COMMUNICATIONS

Published on Web 03/24/2009

Facile Preparation of Highly-Scattering Metal Nanoparticle-Coated Polymer Microbeads and Their Surface Plasmon Resonance

Jung-Hyun Lee,[†] Mahmoud A. Mahmoud,[‡] Valerie Sitterle,[§] Jeffrey Sitterle,[§] and J. Carson Meredith*,[†]

School of Chemical and Biomolecular Engineering, Georgia Institute of Technology, 311 Ferst Drive, Atlanta, Georgia 30332-0100, School of Chemistry and Biochemistry, Georgia Institute of Technology, 901 Atlantic Drive, Atlanta, Georgia 30332-0400, and Georgia Tech Research Institute, Georgia Institute of Technology, 250 14th Street NW, Atlanta, Georgia 30332-0817

Received January 28, 2009; E-mail: carson.meredith@chbe.gatech.edu

Noble-metal coated polymer composite microspheres and nanoshells have attracted intense interest due to applications in electronics, photonics, medical imaging, drug delivery, and catalysis.[1] The light scattering characteristics of large noble metal nanoparticles (NPs) (<140 nm) enables their use as fluorescent analogues.[2] By incorporating such NPs exhibiting preferential scattering characteristics on a polymeric bead surface, such as polystyrene (PS), the composite microsphere can be used as a scattering contrast agent for medical imaging, for optical encoding of biomolecules for sensors and immunoassays, and other optical and electronic devices.[3]

Recent efforts have focused on fabricating such metal-coated polymer composite microspheres. In-situ metal reduction on polymer beads has been reported,[4,5] which usually results in irregular and low metal coverage. Alternatively, techniques for attaching metal NPs to functionalized polymer microspheres have been proposed.[6] Unfortunately metal surface coverage less than 30% is usually reported. Other methods, such as metal NP infiltration and layer-by-layer (LbL) assembly have been utilized.[7−11] The LbL technique results in uniform metal layers, but at the expense of time-consuming sequential deposition cycles. These assemblies may also be unstable in solutions with different pH or ionic-strength.[10,11] The above considerations fuel the demand for more facile methods for incorporation of robust metal NP coatings onto polymeric substrates.

Here, we report a solvent-controlled swelling and heterocoagulation method for preparation of highly scattering metal NP-coated PS latex beads. Metal NPs with different sizes (30, 60, and 80 nm), chemistries (Au and Ag), and shapes (sphere and cube) were successfully coated on unfunctionalized PS beads by the simple addition and removal of a solvent in aqueous cosuspension. The metal coverage, morphology, and optical characteristics were controllable by the organic solvent concentration and the NP concentration, chemistry, shape, and size. This methodology overcomes above-mentioned limitations of previous techniques for preparation of metal-coated dielectrics.

Starting with an aqueous dispersion of PS beads (10 μm diameter) and poly(vinyl pyrrolidone) (PVP)-capped metal (Au or Ag) NPs, homogeneous and dense metal coatings were obtained by the controlled addition and removal of 50 vol % tetrahydrofuran (THF). The resulting composite beads were stable with no loss of the NP coating during long-term (6 months) deionized water storage. Complete and close-packed metal coatings were obtained with smaller and spherical AuNPs, whereas coverage was less complete with larger spheres or cubic NPs.

Figures 1a and 1b show SEM (top) and dark field images (bottom) of the 30 nm AuNPs-coated PS beads. Metal surface coverage increased up to 89% as NP concentration increased (Figure 1b). Dark field microscopy demonstrated that brighter images resulted from the enhanced scattering characteristics of beads with higher metal surface coverage (Figure 1a,b). Atomic force microscopy indicated that the AuNP coating consisted of 1 to ~3 dense NP layers (see Supporting Information).

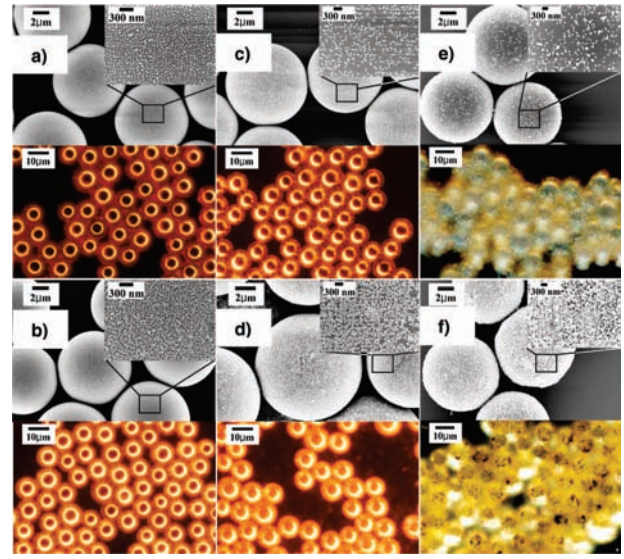

Figure 1. SEM (top) and dark field images (bottom) of 10 μm PS beads covered with metal NPs: (a) 30 nm AuNPs (n = the ratio of the number of metal NPs to PS particles = 2.5×10^5), (b) 30 nm AuNPs ($n = 9.8 \times 10^5$), (c) 80 nm AuNPs ($n = 1.0 \times 10^5$), (d) 80 nm AuNPs ($n = 4.0 \times 10^5$), (e) 60 nm AgNCs ($n = 1.0 \times 10^9$), (f) 60 nm AgNCs ($n = 3.5 \times 10^9$).

Low metal surface coverage (<30%) is commonly reported for direct adsorption of metal NPs from aqueous media.[12] Electrostatic repulsion of the NPs has proven to be the major difficulty in producing dense coatings.[7] The dense coating obtained by the current THF−water technique appears to result from a judicious choice of NP capping agent and the organic solvent added. In our system, the NPs are not charged, but rather are stabilized by the neutral PVP polymer layer. THF drives the swelling of PS and simultaneously induces heteroaggregation of the PVP−NPs and PS particles.[11] The metal capping polymer, PVP, is readily soluble in water but almost insoluble in THF.[13] Hence, the effectiveness of PVP as a polymeric stabilizer is diminished as the composition of THF "nonsolvent" increases. In addition, the PS beads swell reversibly up to 1.5 times their original size by adding 50 vol % THF to water (Supporting Information). During THF removal, NPs adsorbed to the PS bead surface become more compacted as the bead shrinks, leading to increased surface coverage.

In the absence of PS beads, the addition of 50 vol % THF caused the AuNP plasmon peak in the solution to become increasingly red-shifted,

[†] School of Chemical and Biomolecular Engineering.
[‡] School of Chemistry and Biochemistry.
[§] Georgia Technical Research Institute.

10.1021/ja900698w CCC: $40.75

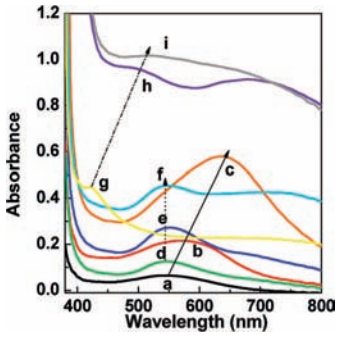

Figure 2. UV−vis spectra of single PS beads coated by metal NPs with different levels of metal coverage. Curves a−c (along the solid line): coated by 30 nm AuNPs. Curves d−f (along the dotted line): coated by 80 nm AuNPs. Curves g−i (along the dash-dot line): coated by 60 nm AgNCs. Metal surface coverage increases along each line. The spectra b, c, d, f, g, and i correspond to the beads in Figure 1 panels a, b, c, d, e, and f, respectively. (Spectra were obtained by subtracting that of a bare PS bead to see altered optical properties of the PS beads by metal coating.)

broadened, and decreased in intensity, indicating aggregation of AuNPs. In contrast, in the presence of PS beads the plasmon peak shows no red-shifting (Supporting Information). Successive decreases in plasmon peak intensity were observed after 1 and 3 h, and a clear supernatant solution with no detectable plasmon peak was obtained after 6 h, indicating essentially complete incorporation of AuNPs onto the PS.

Together with the SEM evidence (Figure 1), these results suggest that the AuNPs aggregate on the surface of the swollen PS beads, rather than in solution. At lower THF fractions AuNPs were too stable, leading to low surface coverage. In fact, no deposition of AuNPs was observed for THF fractions less than 25 vol % after 24 h. This trend did not change significantly over the ratio of NP to PS particles investigated here. THF concentration not only influences NP stability and surface coverage, but also the coating morphology. THF compositions above 50 vol % lead to highly irregular metal coatings, probably caused by direct AuNP aggregation occurring prior to heteroaggregation with the PS beads.

Once AuNPs were incorporated onto the PS bead surface they did not readily detach after applying sonication, washing with water or THF-water solution, or storing in deionized water for 6 months. These results suggest a strong anchoring of metal NPs on the bead surface that is probably mediated by entanglement of the PVP (from the AuNP surface treatment) with glassy PS, during the cycle of PS swelling and shrinking.[15]

Larger size AuNPs (80 nm) and silver nanocubes (AgNCs, 60 nm) were also successfully deposited on PS beads. Surface coverage was controllable in these cases too, indicated by an increase from 27% to 63% (AuNPs, Figure 1c,d) and from 16% to 82% (AgNCs, Figure 1e,f) as NP concentration was increased. Even at the lower surface coverage, bright images of 80 nm AuNP and 60 nm AgNC-coated PS beads were observed in dark field microscopy due to the highly scattering nature of larger AuNPs and cubic AgNCs.

UV−vis absorption spectra from single beads are shown in Figure 2. For the 30 nm AuNP-coated PS bead, the plasmon resonance peak was red-shifted from 580 to 680 nm, the scattering intensity increased, and significant broadening of the plasmon resonance was observed as metal surface coverage increased (curves a−c, along solid line). Surface plasmon coupling and electron−phonon interactions between aggregated NPs are responsible for the broadening of the surface plasmon resonance. The spectra (curve c) of 30 nm Au-coated beads with the highest coverage show the same plasmon resonance wavelength as complete Au shells.[5,8] For the PS bead coated with 80 nm AuNPs, an absorption spectrum with one peak (∼548 nm) was observed for the lowest metal coverage (curve d). As metal surface coverage increased, a broad plasmon peak appeared at longer wavelengths (700−750 nm) due to aggregated AuNPs (shown in Figure 1d), and intensity continued to increase with surface coverage (curves d−f, along dotted line). For the 60 nm AgNC-coated PS bead, the plasmon resonance peak appeared at about 420 nm (curve g). For higher Ag coverage, a significant increase in the scattering intensity, and a broadening of the plasmon resonance were observed, and are assumed to be related to plasmon coupling due to aggregation of AgNCs on the bead surface, shown in Figure 1f. (curves g−i, along dash−dot line).

In conclusion, metal (Au or Ag)-coated PS latex beads have been prepared by a simple solvent (THF)-controlled swelling and heteroaggregation technique. Different sizes, chemistries, and shapes of metal NPs can be coated densely on commercially available PS beads. The resulting composite beads were stable without loss of the metal coating during long-term water storage. The morphology and coverage of the metal coating on the beads, and thus optical properties, were controllable by adjusting the solvent and NP concentrations and the metal NP chemistry, shape, and size.

Acknowledgment. This work was partially supported by NSF Grant CHE 0554668. The authors thank M. El-Sayed for useful discussions, L. Rodeman and M. Mackey for experimental assistance, and M. Srinivasarao for use of the UV−vis microspectrometer.

Supporting Information Available: Experimental details, supplementary UV−vis spectra, AFM image, and optical microscopy. This material is available free of charge via the Internet at http://pubs.acs.org.

References

(1) (a) Kubo, S.; Diaz, A.; Tang, Y.; Mayer, T. S.; Khoo, I. C.; Mallouk, T. E. *Nano Lett.* **2007**, *7*, 3418–3423. (b) Kityk, I. V.; Ebothe, J.; Fuks-Janczarek, I.; Umar, A. A.; Kobayashi, K.; Oyama, M.; Sahraoui, B. *Nanotechnology* **2005**, *16*, 1687–1692. (c) Lee, J. H.; Kim, D. O.; Song, G. S.; Lee, Y.; Jung, S. B.; Nam, J. D. *Macromol. Rapid Commun.* **2007**, *28*, 634–640. (d) Hirsch, L. R.; Jackson, J. B.; Lee, A.; Halas, N. J.; West, J. *Anal. Chem.* **2003**, *75*, 2377–2381.
(2) Yguerabide, J.; Yguerabide, E. E. *Anal. Biochem.* **1998**, *262*, 137–156.
(3) (a) Chen, J.; Saeki, F.; Wiley, B. J.; Cang, H.; Cobb, M. J.; Li, Z. Y.; Au, L.; Zhang, H.; Kimmey, M. B.; Li, X. D.; Xia, Y. *Nano Lett.* **2005**, *5*, 473–477. (b) Siiman, O.; Jitianu, A.; Bele, M.; Grom, P.; Matijevic, E. *J. Colloid Interface Sci.* **2007**, *309*, 8–20.
(4) (a) Jana, S.; Pande, S.; Panigrahi, S.; Praharaj, S.; Basu, S.; Pal, A.; Pal, T. *Langmuir* **2006**, *22*, 7091–7095. (b) Jana, S.; Ghosh, S. K.; Nath, S.; Pande, S.; Praharaj, S.; Panigrahi, S.; Basu, S.; Endo, T.; Pal, T. *Appl. Catal., A* **2006**, *313*, 41–48. (c) Peceros, K. E.; Xu, X. D.; Bulcock, S. R.; Cortie, M. B. *J. Phys. Chem. B* **2005**, *109*, 21516–21520. (d) Chen, C. W.; Serizawa, T.; Akashi, M. *Chem. Mater.* **1999**, *11*, 1381–1389.
(5) Zhang, J. H.; Liu, J. B.; Wang, S. Z.; Zhan, P.; Wang, Z. L.; Ming, N. B. *Adv. Funct. Mater.* **2004**, *14*, 1089–1096.
(6) (a) Shi, W. L.; Sahoo, Y.; Swihart, M. T.; Prasad, P. N. *Langmuir* **2005**, *21*, 1610–1617. (b) Phadtare, S.; Kumar, A.; Vinod, V. P.; Dash, C.; Palaskar, D. V.; Rao, M.; Shukla, P. G.; Sivaram, S.; Sastry, M. *Chem. Mater.* **2003**, *15*, 1944–1949. (c) Cao, Y. C.; Hua, X. F.; Zhu, X. X.; Wang, Z.; Huang, Z. L.; Zhao, Y. D.; Chen, H.; Liu, M.-X. *J. Immunol. Methods* **2006**, *317*, 163–170. (d) Kaltenpoth, G.; Himmelhaus, M.; Slansky, L.; Caruso, F.; Grunze, M. *Adv. Mater.* **2003**, *15*, 1113–1118.
(7) Gittins, D. I.; Susha, A. S.; Schoeler, B.; Caruso, F. *Adv. Mater.* **2002**, *14*, 508–512.
(8) Ji, T. H.; Lirtsman, V. G.; Avny, Y.; Davidov, D. *Adv. Mater.* **2001**, *13*, 1253–1256.
(9) (a) Liang, Z. J.; Susha, A.; Caruso, F. *Chem. Mater.* **2003**, *15*, 3176–3183. (b) Caruso, F.; Lichtenfeld, H.; Giersig, M.; Mohwald, H. *J. Am. Chem. Soc.* **1998**, *120*, 8523–8524. (c) Kato, N.; Caruso, F. *J. Phys. Chem. B* **2005**, *109*, 19604–19612. (d) Cassagneau, T.; Caruso, F. *Adv. Mater.* **2002**, *14*, 732–736. (e) Liang, Z. J.; Susha, A. S.; Caruso, F. *Adv. Mater.* **2002**, *14*, 1160–1164.
(10) Furusawa, K.; Velev, O. D. *Colloids Surf., A* **1999**, *159*, 359–371.
(11) Radtchenko, I. L.; Sukhorukov, G. B.; Gaponik, N.; Kornowski, A.; Rogach, A. L.; Mohwald, H. *Adv. Mater.* **2001**, *13*, 1684–1687.
(12) (a) Dokoutchaev, A.; James, J. T.; Koene, S. C.; Pathak, S.; Prakash, G. K. S.; Thompson, M. E. *Chem. Mater.* **1999**, *11*, 2389–2399. (b) Caruso, F. *Adv. Mater.* **2001**, *13*, 11–22.
(13) Graf, C.; Vossen, D. L. J.; Imhof, A.; van Blaaderen, A. *Langmuir* **2003**, *19*, 6693–6700.
(14) (a) Smith, J. N.; Meadows, J.; Williams, P. A. *Langmuir* **1996**, *12*, 3773–3778. (b) Lee, J. M.; Kim, D. W.; Lee, Y. H.; Oh, S. G. *Chem. Lett.* **2005**, *34*, 928–929.
(15) Kim, A. J.; Manoharan, V. N.; Crocker, J. C. *J. Am. Chem. Soc.* **2005**, *127*, 1592–1593.

JA900698W